CRYSTAL GROWTH & DESIGN

pubs.acs.org/crystal

Article

Natural Antimicrobials Meet a Synthetic Antibiotic: Carvacrol/Thymol and Ciprofloxacin Cocrystals as a Promising Solid-State Route to Activity Enhancement

Oleksii Shemchuk, Simone d'Agostino, Cecilia Fiore, Vittorio Sambri, Silvia Zannoli, Fabrizia Grepioni, and Dario Braga*

Cite This: *Cryst. Growth Des.* 2020, 20, 6796−6803

Read Online

ACCESS | Metrics & More | Article Recommendations | Supporting Information

ABSTRACT: The antibiotic ciprofloxacin (CIP) zwitterion has been cocrystallized via slurry and/or ball-milling with carvacrol (CAR) and thymol (THY), also known to exert antimicrobial activity, with the aim of improving the antibacterial activity of ciprofloxacin. In the case of CAR, the 1:4 cocrystal CIP·CAR_4 appears to be the most stable phase, where the intermediate phases CIP·CAR_3 and CIP·CAR_2 have been isolated by stepwise loss of CAR. In the case of THY, the 1:2 cocrystal CIP·THY_2 is the most stable, while the 1:4 cocrystal CIP·THY_4 easily loses THY to yield the bisadduct. All cocrystals were structurally characterized by single crystal or powder diffraction: in both cocrystals sheets of CIP molecules are intercalated with layers of CAR and THY, respectively, that can be released stepwise upon heating as followed by DSC, TGA and variable temperature XRPD. Preliminary antimicrobial experiments provide encouraging evidence of the enhanced activity of the cocrystals CIP·CAR_4 and CIP·THY_2 against *Escherichia coli* (ATCC 25922) with respect to pure ciprofloxacin as well as to physical mixtures of ciprofloxacin with carvacrol or thymol.

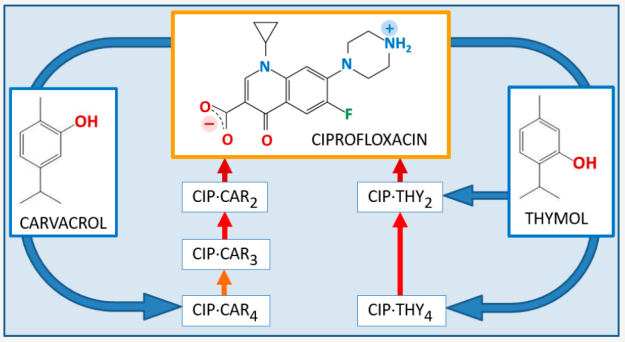

INTRODUCTION

Cocrystallization, an application of crystal engineering principles,[1−5] provides alternative routes to the synthesis of new materials and/or to the enhancement of the properties of active molecules.[6−11] As a matter of fact, cocrystals are finding applications in diverse areas: pharmaceuticals,[12−16] agrochemistry,[17−20] high-energy materials,[21−23] food,[24−26] etc. The basic idea is that the solid state association, via noncovalent interactions, of an active ingredient with a molecular component may alter in a useful way physicochemical properties such as solubility, dissolution rate, thermal stability, photoreactivity, etc. of the active ingredient. Cocrystals have become especially attractive in the pharmaceutical field, since they can lead to new pharmaceutical formulations compared, for example, to conventional salts.

This goal is usually pursued by cocrystallizing the API with a nonactive (GRAS accepted[27]) molecule, as in molecular cocrystals, or with a salt, as in ionic cocrystals.[28] The large choice of molecular and/or ionic building blocks makes the number of possible combinations between active pharmaceutical ingredients (APIs) and ancillary coformers virtually limitless.

In more advanced applications, however, the API may also be cocrystallized with another active ingredient, yielding a so-called codrug,[29−33] whereby not only are the solid state physicochemical properties of the API altered with respect to those of the pure crystal but also the pharmaceutical and biological activity may give significantly different results.[34−36]

In this paper, we apply cocrystallization strategies to approach a problem of extraordinary contemporary importance, namely that of "antimicrobial resistance" (AMR). As a matter of fact, the AMR phenomenon is one of the major medical challenges in most healthcare systems, both in developed countries and in low financial income areas.[37] AMR has increased dramatically in the recent years and represents a global public health threat.[38] A number of diseases that were thought to be under control by the application of antibacterial remedies are getting back being resistant to these therapies. One of the main reasons for *drug*-resistance in microorganisms is the intensive overuse of treatments to control infections in humans and animals as well as in the agricultural sector.[39] Actually, the reason AMR is a significant

Received: June 30, 2020
Revised: August 21, 2020
Published: August 21, 2020

concern is the high mortality level attributed to infections caused by multi drug resistant germs.[40] A number of common pathogenic strains are already bearing antibiotic-resistant genes, and presumably, more antibiotic-resistant pathogens will emerge in the future, if no different and more cautious use of antimicrobials takes place.[41]

To cope with the problem of AMR, two possible strategies can be used: the first is the quest for novel active ingredients, but this is facing increasing bench-to-market costs and times;[42] the second is the exploration of ways to improve the activity of existing antibacterials, and it is more promising. In a recent paper, we showed that cocrystallization of the antibacterial agents proflavine and methyl viologen with the inorganic salts CuCl, $CuCl_2$, and $AgNO_3$ results in enhanced antimicrobial activity with respect to the separate components.[43]

In this paper we report our results in the cocrystallization of the known antibiotic ciprofloxacin (CIP hereafter) with the natural antimicrobials carvacrol (CAR) and thymol (THY) (see Scheme 1). At ambient conditions THY is a molecular solid (mp 51.5 °C),[44] while carvacrol is a liquid (mp 3.5 °C);[44] therefore, crystalline solids containing ciprofloxacin and this latter coformer should be strictly regarded as "pharmaceutical solvates".[45−47] However, as it will be apparent in the following, the distinction between cocrystals and solvates is rather semantic in the contest of this study and does not reflect specific differences in physicochemical behaviors.

Scheme 1. Ciprofloxacin (CIP) Zwitterion and the Two Antimicrobial Molecules, Carvacrol (CAR) and Thymol (THY), Used as Coformers

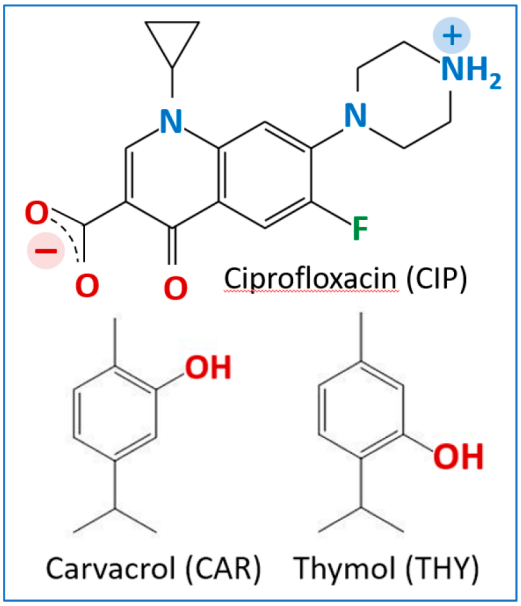

Ciprofloxacin (1-cyclopropyl-6-fluoro-1,4-dihydro-4-oxo-7-(1-piperazinyl)-3-quinoline carboxylic acid) is an antibiotic belonging to the class of fluoroquinolones, which are effective antibacterial agents against a broad spectrum of Gram-positive and Gram-negative bacteria. Thymol [5-methyl-2-(propan-2-yl)benzenol, also known as *m*-thymol] is a natural monoterpenoid phenol derivative of *p*-cymene, and it is the most abundant component of the oil extracted from *Thymus vulgaris* (thyme). Carvacrol [2-methyl-5-(propan-2-yl)benzenol, also known as *o*-thymol], is present in the essential oils of *Origanum vulgare* (oregano), thyme, pepperwort, and wild bergamot. The effective antibacterial properties of both essential oils have been investigated *in vitro* and *in vivo* against diverse Gram-negative and Gram-positive bacteria such as *Salmonella typhimurium*, *Escherichia coli*, and *Listeria monocytogenes*.[48−52] Both THY and CAR are generally used as natural preservatives in food treatment and packaging.[53−56] They are both components of "Thymi aetheroleum", a herbal medicinal product,[57] and have been assigned the GRAS (generally recognized as safe) status of flavor additives[58] by FEMA.[59] Recently cocrystals of thymol and carvacrol, among a number of essential oils components, have been investigated for agricultural applications.[60]

In the following, we describe preparation, solid state characterization and thermal behavior of the two families of ciprofloxacin cocrystals with carvacrol, CIP·CAR_n (n = 2, 3, 4) and with thymol, CIP·THY_n (n = 2, 4). The effect of cocrystals formation on the antibiotic activity of ciprofloxacin has also been evaluated by means of standard antimicrobial tests in the case of CIP·CAR_4 and CIP·THY_2 and compared with the results for the pure components and their physical mixtures. Preliminary results are encouraging, and they have prompted a thorough antimicrobial investigation, which will be the subject of a separate research project.

EXPERIMENTAL PART

Materials and Instrumentation. All reagents and solvents used in this work were purchased from Sigma-Aldrich and used without further purification.

Synthesis of Ciprofloxacin Cocrystals with Carvacrol. *CIP·CAR_4.* CIP·CAR_4 was obtained by three different methods: solution, mechanochemistry, and slurry. In the first one, ciprofloxacin (30 mg, 0.09 mmol) was dissolved in carvacrol (2 mL, 12.99 mmol), and upon solvent evaporation single crystals were obtained after 2 weeks. In the second one, 100 mg (0.30 mmol) of ciprofloxacin were manually ground with 4−5 drops of carvacrol, added in a stepwise manner: the powder was ground until dryness, and then an additional drop of CAR was added. In the third method, ciprofloxacin was slurried for 60 h in 3 mL of ethanol with a slight excess of carvacrol with respect to the CIP:CAR 1:4 stoichiometric ratio; after filtration, the solid material was left to dry out at room temperature.

CIP·CAR_3. CIP·CAR_3 was obtained in two steps starting from CIP·CAR_4: first CIP·CAR_4 was heated to 80 °C in an oven and kept at this temperature for 30 min; the sample was then cooled to 40 °C and kept at this temperature for 4 h.

CIP·CAR_2. CIP·CAR_2 was obtained in two steps starting from CIP·CAR_4: first CIP·CAR_4 was heated to 100 °C in an oven and kept at this temperature for 30 min; the sample was then cooled to 40 °C and kept at this temperature for 4 h.

All attempts to synthesize CIP·CAR_2 and CIP·CAR_3 by direct mixing of the reactants in the correct stoichiometric ratios were unsuccessful.

Synthesis of Ciprofloxacin Cocrystals with Thymol. *CIP·THY_2.* CIP·THY_2 was obtained mechanochemically by ball milling ciprofloxacin (100 mg, 0.30 mmol) and thymol (90.7 mg, 0.60 mmol) for 30 min in a Retsch MM200 ball miller, operated at a frequency of 20 Hz, in the presence of 2 drops (100 μL) of ethanol.

CIP·THY_4. A solid mixture of ciprofloxacin (30 mg, 0.09 mmol) and thymol (150 mg, 1.00 mmol) was gently ground and subsequently heated to 55 °C, to induce the melting of thymol (mp of 51.5 °C).[44] Upon slow cooling the growth of single crystals was observed. CIP·THY_4 was also obtained via slurry: ciprofloxacin (100 mg, 0.30 mmol) and excess thymol (272 mg, 1.80 mmol) were slurried in 2 mL of ethanol for 60 h in a closed vial; the vial was then opened, still under slurry conditions, to allow the complete evaporation of ethanol.

Thermogravimetric Analysis (TGA). TGA measurements (Figures SI-6 to SI-11) for all compounds were performed with a

https://dx.doi.org/10.1021/acs.cgd.0c00900
Cryst. Growth Des. 2020, 20, 6796−6803

PerkinElmer TGA7 in the temperature range 30−400 °C, under an N_2 gas flow, at the heating rate of 5 °C min^{-1}.

Differential Scanning Calorimetry (DSC). DSC measurements (Figures SI-12 to SI-16) for all compounds were performed with a Perkin−Elmer Diamond, at the heating rate of 5 °C min^{-1}. Samples (3−5 mg) were placed in hermetic aluminum pans.

X-ray Powder Diffraction Measurements. Room temperature X-ray powder diffraction (XRPD) patterns were collected on a PANalytical X'Pert Pro automated diffractometer equipped with an X'Celerator detector in Bragg−Brentano geometry, using Cu Kα radiation (λ = 1.5418 Å) without monochromator in the 3−40° 2θ range (step size, 0.033°; time/step, 20 s; Soller slit, 0.04 rad; antiscatter slit, 1/2; divergence slit, 1/4; 40 mA × 40 kV). For structure solution purposes, X-ray diffraction patterns were collected on a PANalytical X'Pert Pro automated diffractometer with transmission geometry equipped with a focusing mirror and Pixcel detector, using Cu Kα radiation (λ = 1.5418 Å) without monochromator in the 2θ range 3−70° (step size, 0.0130°; time/step, 170.595 s; Soller slit, 0.04 rad; antiscatter slit, 1/2; divergence slit, 1/2; 40 kV × 40 mA). To improve the quality of the obtained XRPD patterns, three repetitions were performed, and the scans were merged. Data analyses were carried out using the PANalytical X'Pert Highscore Plus program.[61]

Structural Characterization from Powder Data. Powder diffraction data were analyzed with the software PANalytical X'Pert HighScore Plus. Fifteen peaks were chosen in the 2θ range 3−40°, and unit cell parameters were found using the DICVOL4 algorithm. The structure of CIP·THY_2 was solved by simulated annealing, performed with EXPO2014.[62] Ten runs for simulated annealing trials were set, and a cooling rate (defined as the ratio T_n/T_{n-1}) of 0.95 was used. The best solution was chosen for Rietveld refinement, which was performed with the software TOPAS 5.0.[63] The peak shape was modeled for size and strain with the Gaussian and Lorentzian functions present in TOPAS 5.0. All the hydrogen atoms were fixed in calculated positions. Refinement converged with χ^2 = 1.84 and R_{wp} = 6.51%. Rietveld refinement is shown in the Supporting Information (Figure SI-1). Structural data for all compounds investigated in this work are listed in Table SI-1.

Variable Temperature X-ray Diffraction. X-ray powder diffractograms in the 3−40° 2θ range were collected for CIP·CAR_4 and CIP·THY_4 on a PANalytical X'Pert PRO automated diffractometer, equipped with an X'Celerator detector and an Anton Paar TTK 450 system for measurements at controlled temperature. Data were collected in open air in Bragg−Brentano geometry using Cu Kα radiation without a monochromator. Thermal programs were selected on the basis of TGA results.

Single Crystal X-ray Diffraction. Single crystal X-ray diffraction data for CIP·CAR_4 and CIP·THY_4 were collected at room temperature and at 250 K, respectively, with an Oxford Diffraction X'Calibur equipped with a graphite monochromator and a CCD detector. Unit cell parameters for all compounds discussed herein are reported in Table SI-1. The structures were solved by the Intrinsic Phasing methods and refined by least-squares methods against F^2 using SHELXT-2016[64] and SHELXL-2018[65] with $Olex^2$ interface.[66] Non-hydrogen atoms were refined anisotropically. Hydrogen atoms were added in calculated positions. The software Mercury 4.1.2[67] was used to analyze and represent the crystal packing. Crystal data can be obtained free of charge *via* www.ccdc.cam.ac.uk/conts/retrieving.html (or from the Cambridge Crystallographic Data Centre, 12 Union Road, Cambridge CB21EZ, UK; fax: (+44)1223-336-033; or e-mail: deposit@ccdc.cam.ac.uk). CCDC 2010400−2010402.

Testing of Antimicrobial Activity. Antimicrobial activity was tested with broth microdilution, according to the guidelines of the two established organizations and committees on antimicrobial susceptibility testing, the CLSI and EUCAST.[68−70] For comparison, testing was conducted on suspensions of thymol, carvacrol, ciprofloxacin, and both physical mixtures and cocrystals of CIP·THY_2 and CIP·CAR_4, in 10 progressive concentrations ranging from 0.063 to 160 μg mL^{-1}. All suspensions were tested in parallel, using both a reference strain of *E. coli* (ATCC 25922), which is susceptible to ciprofloxacin, and a ciprofloxacin-resistant *E. coli* strain (MIC > 32).[70]

RESULTS AND DISCUSSION

Cocrystals of Ciprofloxacin with Carvacrol. The cocrystallization of ciprofloxacin with CAR resulted in the formation of the cocrystal CIP·CAR_4, characterized by a 1:4 stoichiometry. Figure 1a shows how the carboxylate group on

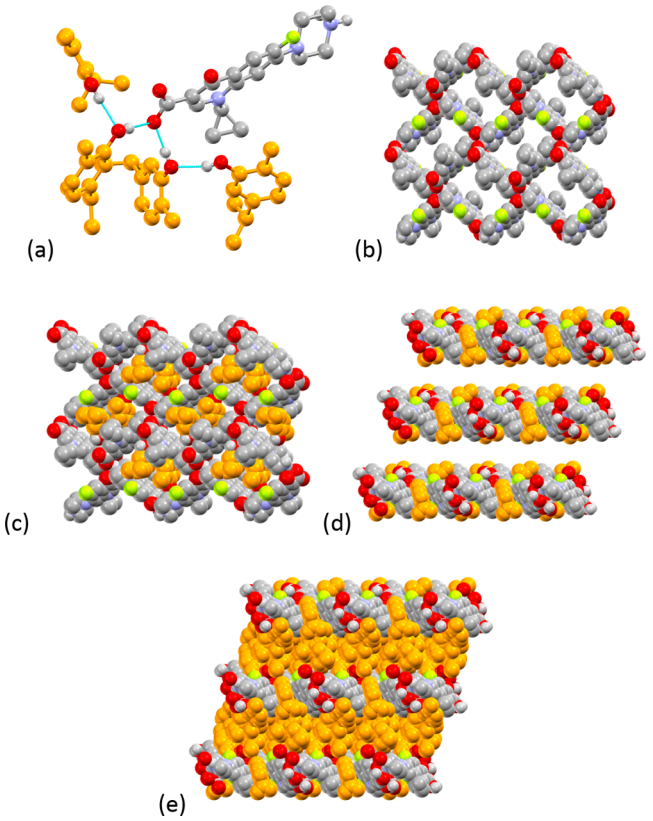

Figure 1. Hydrogen-bonding interactions between ciprofloxacin and the carvacrol molecules in crystalline CIP·CAR_4 (a). The ciprofloxacin molecules also interact with each other via hydrogen bonds; they are arranged in nets (b) filled with a quarter of the CAR molecules (c), thus forming parallel layers (d) alternating with thick layers of CAR molecules (e). H_{CH} hydrogens were omitted for clarity. Carbon atoms of CAR are given in orange.

ciprofloxacin interacts via hydrogen bonds with the −OH group of two molecules of CAR, while the remaining two CAR molecules in the formula unit form OH···O_{OH} hydrogen bonds with other CAR molecules. Each ciprofloxacin molecules interacts via NH^+···O_{COO^-} and COO^-···HN^+ hydrogen bonds with four neighboring ciprofloxacin molecules. Figure 1c shows an interesting feature of the molecular packing in crystals of CIP·CAR_4, namely a layered structure: one layer is formed by ciprofloxacin and two (referred by symmetry) CAR molecules, while the second layer is exclusively formed by the remaining three CAR molecules. This feature is of help in understanding the thermal behavior of the cocrystal (see below), and it is shared with the cocrystal of ciprofloxacin with THY. Segregation of CAR and THY has also been observed in cocrystals with acridine.[71]

The study of the thermal behavior of CIP·CAR_4 via DSC allows one to observe, on heating, the presence of multiple endothermic events at 80, 92, and 109 °C (peak temperatures,

https://dx.doi.org/10.1021/acs.cgd.0c00900
Cryst. Growth Des. 2020, 20, 6796−6803

see Figure SI-7), followed by exothermic events. This is an indication that CAR molecules are released stepwise from the crystal, and each loss of CAR is immediately followed by recrystallization to a cocrystal with different stoichiometry. The last step corresponds to complete loss of CAR and recrystallization of ciprofloxacin. The stepwise loss of CAR from CIP·CAR_4 to CIP is summarized in Scheme 2.

Scheme 2. Solid-State Transformations upon Heating for the 1:4 Cocrystals of Ciprofloxacin (CIP) Zwitterion with Carvacrol (CAR) and Thymol (THY)[a]

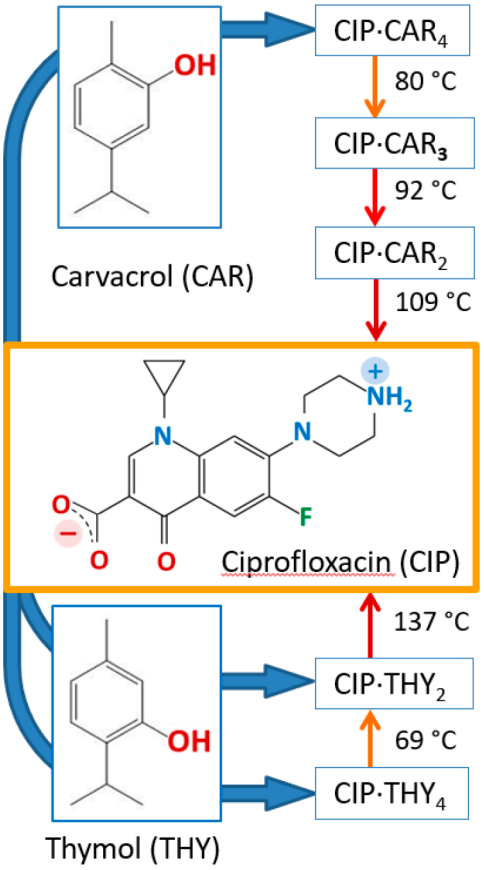

[a]Temperatures are from DSC measurements (peak values, see Supporting Information).

The series of solid-to-solid transformations occurring upon heating crystalline CIP·CAR_4 was also followed by variable temperature X-ray powder diffraction (see Figure SI-3). The temperatures at which the transformations occur from CIP·CAR_4 to CIP·CAR_3, then to CIP·CAR_2 and finally to CIP, are in agreement (80, 100, and 110 °C, respectively) with the DSC values. Thermal gravimetric analysis, on the contrary, is not as informative (see Figure SI-13), and its trace shows a single, broad event corresponding to the loss of all CAR molecules per formula unit (weight loss ca. 63%) in the temperature range 60−150 °C. This is attributable to the low volatility of CAR, which leaves the crystal but does not evaporate from the sample in the TGA experiment. VT-XRPD experiments confirmed this observation: two samples of CIP·CAR_4 were first converted into CIP·CAR_3 and CIP·CAR_2, respectively, and then they were cooled to room temperature. In both cases, partial reformation of CIP·CAR_4 could be observed; i.e., excess of CAR was still available in the powder samples at the end of the heating cycles.

The results of the VT-XRPD measurements were useful for the preparation of the intermediate phases CIP·CAR_2 and CIP·CAR_3 as pure materials. In both cases samples of CIP·CAR_4 were heated to the transition temperatures (ca. 80 and 100 °C, respectively) and kept at these temperatures for 30 min, to allow for complete transformation; the samples were then cooled to 40 °C and kept at this temperature for 3−4 h to allow for complete evaporation of the excess CAR. TGA measurements on these pure samples (see Figures SI-15 and SI-16) allowed to confirm the CIP·CAR_3 and CIP·CAR_2 stoichiometries. Once formed, all cocrystals of ciprofloxacin with CAR are stable. Even after 50 days in the open air, no change of crystalline phase was observed.

Cocrystals of Ciprofloxacin with Thymol. Thymol is a solid at ambient conditions, but it melts at 51.5 °C.[44] For this reason, the same cocrystallization approach used for ciprofloxacin with CAR was applied here, and ciprofloxacin was dissolved in excess melted THY (see Experimental Part). Upon slow cooling of the mixture two types of single crystals were recovered, and both were characterized via X-ray single crystal diffraction. The first type of crystals turned out to be pure THY, identified on the basis of CSD data (refcode IPMEPL[72]), while crystals of the second type were characterized as the new cocrystal CIP·THY_4. Data were collected at 250 K, to avoid loss of THY during data collection. In terms of crystal structure, CIP·THY_4 closely resembles CIP·CAR_4, as is evident from Figure 2.

Figure 2a shows how ciprofloxacin interacts via hydrogen bonds with the −OH group of three molecules of THY, while the remaining THY molecules in the formula unit form an $OH\cdots O_{OH}$ hydrogen bond with another THY molecule. As observed in CIP·CAR_4, each ciprofloxacin molecules interacts via hydrogen bonds with four neighboring ciprofloxacin molecules, thus forming a 2D-net (see Figure 2b) filled with THY molecules (Figure 2c). The most relevant analogy, however, is represented by the layered organization, as thick layers of THY intercalate between the ciprofloxacin/THY layers, as shown in Figures 2, part d and e.

Ciprofloxacin and THY were also made to mechanochemically react in 1:4 stoichiometric ratio in a ball milling experiment, in the presence of two drops of ethanol. This time, however, a new solid was obtained, characterized by a powder diffraction pattern different from those of the starting materials and of CIP·THY_4, although peaks of unreacted THY were still present. The synthesis via ball milling was thus repeated with lower quantities of THY, and a pure phase was obtained with the 1:2 stoichiometric ratio, as confirmed by TGA (see Figure SI-14). The new cocrystal CIP·THY_2 was structurally characterized from powder data (see Experimental Part), since all attempts to grow single crystals were unsuccessful. Figure 3a shows the hydrogen-bonding interactions of ciprofloxacin with the two independent THY molecules. As in CIP·THY_4 the CIP molecules form a 2D net (Figure 3b), with ciprofloxacin molecules connected via hydrogen bonds; parallel nets (Figure 3c) are intercalated with THY molecules, which also partially enter the CIP layers with the −OH groups (Figure 3d).

Pure CIP·THY_4 was also obtained by slurry in EtOH with an excess of THY; the resulting solid was then left in the air for 72 h, for the excess of THY to sublimate. A DSC measurement on CIP·THY_4 thus obtained (Figure SI-8) shows two endother-

https://dx.doi.org/10.1021/acs.cgd.0c00900
Cryst. Growth Des. 2020, 20, 6796−6803

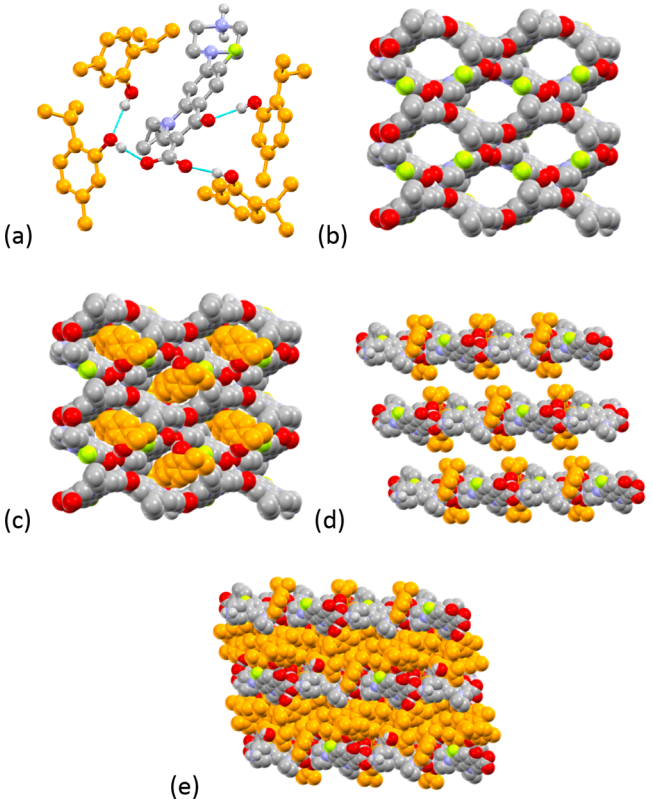

Figure 2. Hydrogen-bonding interactions between ciprofloxacin and the thymol molecules in crystalline CIP·THY_4 (a). The ciprofloxacin molecules also interact with each other via hydrogen bonds; they are arranged in nets (b) filled with a quarter of the THY molecules (c), thus forming parallel layers (d) alternating with thick layers of THY molecules (e). H_{CH} hydrogens were omitted for clarity. Carbon atoms of THY are given in orange.

mic events, at ca. 69 °C and at 137 °C, respectively. VT-XRPD experiments (Figure SI-5) confirmed that the first event corresponds to the transformation of CIP·THY_4 into CIP·THY_2, while the second one leads to complete loss of THY. The stepwise loss of THY and the thermal transformation of CIP·THY_4, first into CIP·THY_2 and then into CIP, are summarized in Scheme 2.

Antimicrobial Activity. The antimicrobial activity of the cocrystals CIP·CAR_4 and CIP·THY_2, chosen because they could easily be obtained mechanochemically as pure phases, was compared with that of the pure components, as well as with that of physical mixtures of CIP and CAR/THY in adequate stoichiometric ratios, against a reference strain of *E. coli* (ATCC 25922), which is susceptible to the ciprofloxacin component. Pure samples of CIP·CAR_4 and CIP·THY_4 obtained as described above were used.

Concerning strain ATCC 25922, ciprofloxacin showed growth inhibition at 4 μg/mL, while THY and CAR were not effective by themselves and did not show growth inhibition. The physical mixtures of CIP and CAR and of CIP and THY in 1:4 and 1:2 ratios, respectively, resulted in growth inhibition at ca. 10 μg/mL, which, upon normalization, approximately corresponds to the inhibition effect of pure ciprofloxacin. Interestingly, both CIP·CAR_4 and CIP·THY_2 cocrystals showed growth inhibition at ca. 2 μg/mL concentration; normalizing these quantities on the base of the cocrystals formula units, it can be seen that CIP·CAR_4 and CIP·THY_2 are ca. 6 and 4 times more efficient, respectively, with respect to pure ciprofloxacin.

CONCLUSIONS

The study of cocrystals is at the forefront of crystal engineering because it offers a viable route to prepare, often with nonexpensive and environmentally friendly solvent free (mechanochemical) methods, novel materials for a variety of applications well beyond the pharmaceutical field. For instance,

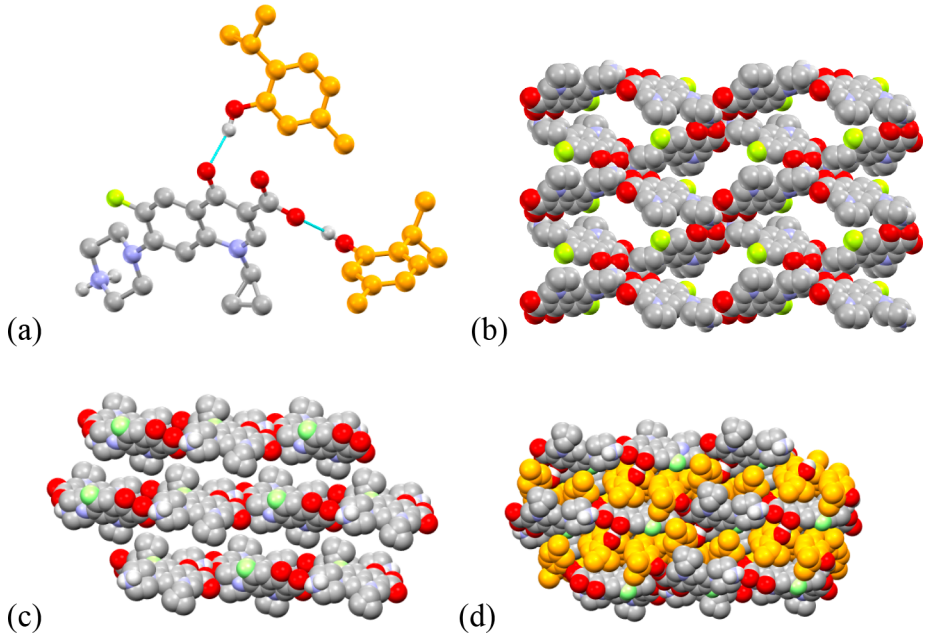

Figure 3. Hydrogen-bonding interactions between ciprofloxacin and the thymol molecules in crystalline CIP·THY_2 (a). As in CIP·THY4, the CIP molecules form 2D-nets (b and c), filled with the −OH extremities of the intercalated thymol layers (d). H_{CH} hydrogens were omitted for clarity. Carbon atoms of THY are given in orange.

https://dx.doi.org/10.1021/acs.cgd.0c00900
Cryst. Growth Des. 2020, 20, 6796−6803

it has been amply shown that cocrystallization approaches can be used to produce materials that can be used as fertilizers, nutrients and enzyme inhibitors in the agrochemical field.[17−19] There are also indications that cocrystals could be used in an area of increasing global importance, such as that of antimicrobial resistance. In the case of proflavine, for example, it has been possible to demonstrate that cocrystallization of proflavine with CuCl and $AgNO_3$ yield materials, namely PF·CuCl and PF·$AgNO_3$ that appear to perform better in terms of antimicrobial activity than proflavine and the inorganic salts, separately.[43]

In this paper, we have reported the preparation and characterization of a series of cocrystals obtained by cocrystallizing by slurry and/or ball-milling the antibiotic ciprofloxacin (CIP) with carvacrol (CAR) and thymol (THY), which are also known to exert antibacterial activity. CIP forms compounds in 1:4 ratio with both coformers. While CIP·CAR_4 is stable and loses CAR in stepwise manner upon heating with formation of the phases CIP·CAR_3 and CIP·CAR_2, while CIP·THY_4 is unstable and loses THY spontaneously at room temperature with formation of stable CIP·THY_2.

The idea was that of verifying whether cocrystallization of a known antibiotic with herbal medicinal products could indeed represent a viable route to improve the properties of ciprofloxacin. Preliminary antimicrobial testing against a reference strain of *E. coli* (ATCC 25922), susceptible to ciprofloxacin, clearly indicated that cocrystals CIP·CAR_4 or CIP·THY_2 have the comparable bacteriostatic activity, and that this is significantly better than ciprofloxacin alone. If one takes into account that THY and CAR appear to be not effective on their own, or in physical mixture with ciprofloxacin, it appears that association with ciprofloxacin in the cocrystals enhances significantly its efficacy. These encouraging preliminary results require an in depth systematic study, which is under way.

■ ASSOCIATED CONTENT

Supporting Information

The Supporting Information is available free of charge at https://pubs.acs.org/doi/10.1021/acs.cgd.0c00900.

XRPD patterns, DSC, and TGA (PDF)

Accession Codes

CCDC 2010400−2010402 contain the supplementary crystallographic data for this paper. These data can be obtained free of charge via www.ccdc.cam.ac.uk/data_request/cif, or by emailing data_request@ccdc.cam.ac.uk, or by contacting The Cambridge Crystallographic Data Centre, 12 Union Road, Cambridge CB2 1EZ, UK; fax: +44 1223 336033.

■ AUTHOR INFORMATION

Corresponding Author

Dario Braga − *Molecular Crystal Engineering Laboratory, Dipartimento di Chimica "Giacomo Ciamician", Università di Bologna, 40126 Bologna, Italy;* orcid.org/0000-0003-4162-4779; Email: dario.braga@unibo.it

Authors

Oleksii Shemchuk − *Molecular Crystal Engineering Laboratory, Dipartimento di Chimica "Giacomo Ciamician", Università di Bologna, 40126 Bologna, Italy;* orcid.org/0000-0003-3003-3922

Simone d'Agostino − *Molecular Crystal Engineering Laboratory, Dipartimento di Chimica "Giacomo Ciamician", Università di Bologna, 40126 Bologna, Italy;* orcid.org/0000-0003-3065-5860

Cecilia Fiore − *Molecular Crystal Engineering Laboratory, Dipartimento di Chimica "Giacomo Ciamician", Università di Bologna, 40126 Bologna, Italy*

Vittorio Sambri − *Dipartimento di Medicina Specialistica, Diagnostica e Sperimentale Università di Bologna, 40138 Bologna, Italy; Laboratorio Unico Centro Servizi AUSL Romagna, U.O. Microbiologia, Pievesestina (FC), Italy*

Silvia Zannoli − *Laboratorio Unico Centro Servizi AUSL Romagna, U.O. Microbiologia, Pievesestina (FC), Italy*

Fabrizia Grepioni − *Molecular Crystal Engineering Laboratory, Dipartimento di Chimica "Giacomo Ciamician", Università di Bologna, 40126 Bologna, Italy;* orcid.org/0000-0003-3895-0979

Complete contact information is available at: https://pubs.acs.org/10.1021/acs.cgd.0c00900

Notes

The authors declare no competing financial interest.

■ ACKNOWLEDGMENTS

Financial support from the University of Bologna is acknowledged. We thank Dr. Katia Rubini for assistance with DSC and TGA measurements.

■ REFERENCES

(1) Desiraju, G. R.; Parshall, G. W. Crystal engineering: the design of organic solids. *Materials science monographs* **1989**, 54.

(2) Almarsson, O.; Zaworotko, M. J. Crystal engineering of the composition of pharmaceutical phases. Do pharmaceutical co-crystals represent a new path to improved medicines? *Chem. Commun.* **2004**, 1889−1896.

(3) Blagden, N.; de Matas, M.; Gavan, P. T.; York, P. Crystal engineering of active pharmaceutical ingredients to improve solubility and dissolution rates. *Adv. Drug Delivery Rev.* **2007**, *59*, 617−630.

(4) Desiraju, G. R. Crystal engineering: a holistic view. *Angew. Chem., Int. Ed.* **2007**, *46*, 8342−8356.

(5) Braga, D.; Grepioni, F.; Maini, L.; d'Agostino, S. Making crystals with a purpose; a journey in crystal engineering at the University of Bologna. *IUCrJ* **2017**, *4*, 369−379.

(6) Aakeroy, C. B.; Salmon, D. J. Building co-crystals with molecular sense and supramolecular sensibility. *CrystEngComm* **2005**, *7*, 439−448.

(7) Babu, N. J.; Nangia, A. Solubility Advantage of Amorphous Drugs and Pharmaceutical Cocrystals. *Cryst. Growth Des.* **2011**, *11*, 2662−2679.

(8) Andre, V.; Shemchuk, O.; Grepioni, F.; Braga, D.; Duarte, M. T. Expanding the Pool of Multicomponent Crystal Forms of the Antibiotic 4-Aminosalicylic Acid: The Influence of Crystallization Conditions. *Cryst. Growth Des.* **2017**, *17*, 6417−6425.

(9) Good, D. J.; Rodriguez-Hornedo, N. Solubility Advantage of Pharmaceutical Cocrystals. *Cryst. Growth Des.* **2009**, *9*, 2252−2264.

(10) Yadav, A. V.; Shete, A. S.; Dabke, A. P.; Kulkarni, P. V.; Sakhare, S. S. Co-crystals: a novel approach to modify physicochemical properties of active pharmaceutical ingredients. *Indian J. Pharm. Sci.* **2009**, *71*, 359−370.

(11) Schultheiss, N.; Newman, A. Pharmaceutical Cocrystals and Their Physicochemical Properties. *Cryst. Growth Des.* **2009**, *9*, 2950−2967.

(12) Golob, S.; Perry, M.; Lusi, M.; Chierotti, M. R.; Grabnar, I.; Lassiani, L.; Voinovich, D.; Zaworotko, M. J. Improving Biopharmaceutical Properties of Vinpocetine Through Cocrystallization. *J. Pharm. Sci.* **2016**, *105*, 3626−3633.

(13) Shan, N.; Zaworotko, M. J. The role of cocrystals in pharmaceutical science. *Drug Discovery Today* **2008**, *13*, 440−446.
(14) Stanton, M. K.; Bak, A. Physicochemical properties of pharmaceutical co-crystals: A case study of ten AMG 517 co-crystals. *Cryst. Growth Des.* **2008**, *8*, 3856−3862.
(15) Steed, J. W. The role of co-crystals in pharmaceutical design. *Trends Pharmacol. Sci.* **2013**, *34*, 185−193.
(16) Wouters, J.; Quéré, L. *Pharmaceutical salts and co-crystals*; Royal Society of Chemistry: 2011.
(17) Honer, K.; Kalfaoglu, E.; Pico, C.; McCann, J.; Baltrusaitis, J. Mechanosynthesis of Magnesium and Calcium Salt−Urea Ionic Cocrystal Fertilizer Materials for Improved Nitrogen Management. *ACS Sustainable Chem. Eng.* **2017**, *5*, 8546−8550.
(18) Casali, L.; Mazzei, L.; Shemchuk, O.; Sharma, L.; Honer, K.; Grepioni, F.; Ciurli, S.; Braga, D.; Baltrusaitis, J. Novel Dual-Action Plant Fertilizer and Urease Inhibitor: Urea·Catechol Cocrystal. Characterization and Environmental Reactivity. *ACS Sustainable Chem. Eng.* **2019**, *7*, 2852−2859.
(19) Julien, P. A.; Germann, L. S.; Titi, H. M.; Etter, M.; Dinnebier, R. E.; Sharma, L.; Baltrusaitis, J.; Friscic, T. In situ monitoring of mechanochemical synthesis of calcium urea phosphate fertilizer cocrystal reveals highly effective water-based autocatalysis. *Chem. Sci.* **2020**, *11*, 2350−2355.
(20) Nauha, E.; Nissinen, M. Co-crystals of an agrochemical active − A pyridine-amine synthon for a thioamide group. *J. Mol. Struct.* **2011**, *1006*, 566−569.
(21) Zhang, J.; Shreeve, J. n. M. Time for pairing: cocrystals as advanced energetic materials. *CrystEngComm* **2016**, *18*, 6124−6133.
(22) Wei, X.; Ma, Y.; Long, X.; Zhang, C. A strategy developed from the observed energetic−energetic cocrystals of BTF: cocrystallizing and stabilizing energetic hydrogen-free molecules with hydrogenous energetic coformer molecules. *CrystEngComm* **2015**, *17*, 7150−7159.
(23) Kent, R. V.; Wiscons, R. A.; Sharon, P.; Grinstein, D.; Frimer, A. A.; Matzger, A. J. Cocrystal Engineering of a High Nitrogen Energetic Material. *Cryst. Growth Des.* **2018**, *18*, 219−224.
(24) Schultheiss, N.; Bethune, S.; Henck, J. O. Nutraceutical cocrystals: utilizing pterostilbene as a cocrystal former. *CrystEngComm* **2010**, *12*, 2436−2442.
(25) Bethune, S. J.; Schultheiss, N.; Henck, J. O. Improving the Poor Aqueous Solubility of Nutraceutical Compound Pterostilbene through Cocrystal Formation. *Cryst. Growth Des.* **2011**, *11*, 2817−2823.
(26) Bevill, M. J.; Vlahova, P. I.; Smit, J. P. Polymorphic Cocrystals of Nutraceutical Compound p-Coumaric Acid with Nicotinamide: Characterization, Relative Solid-State Stability, and Conversion to Alternate Stoichiometries. *Cryst. Growth Des.* **2014**, *14*, 1438−1448.
(27) Burdock, G. A.; Carabin, I. G. Generally recognized as safe (GRAS): history and description. *Toxicol. Lett.* **2004**, *150*, 3−18.
(28) Braga, D.; Grepioni, F.; Lampronti, G. I.; Maini, L.; Turrina, A. Ionic Co-crystals of Organic Molecules with Metal Halides: A New Prospect in the Solid Formulation of Active Pharmaceutical Ingredients. *Cryst. Growth Des.* **2011**, *11*, 5621−5627.
(29) Sekhon, B. S. Drug-drug co-crystals. *Daru, J. Pharm. Sci.* **2012**, *20*, 45.
(30) Braga, D.; Grepioni, F.; Maini, L.; Capucci, D.; Nanna, S.; Wouters, J.; Aerts, L.; Quere, L. Combining piracetam and lithium salts: ionic co-crystals and co-drugs? *Chem. Commun.* **2012**, *48*, 8219−8221.
(31) Bordignon, S.; Cerreia Vioglio, P.; Priola, E.; Voinovich, D.; Gobetto, R.; Nishiyama, Y.; Chierotti, M. R. Engineering Codrug Solid Forms: Mechanochemical Synthesis of an Indomethacin−Caffeine System. *Cryst. Growth Des.* **2017**, *17*, 5744−5752.
(32) Shemchuk, O.; Braga, D.; Grepioni, F. Ionic Cocrystals of Levodopa and Its Biological Precursors L-Tyrosine and L-Phenylalanine with LiCl. *Cryst. Growth Des.* **2019**, *19*, 6560−6565.
(33) Wang, L.-Y.; Bu, F.-Z.; Li, Y.-T.; Wu, Z.-Y.; Yan, C.-W. A Sulfathiazole−Amantadine Hydrochloride Cocrystal: The First Codrug Simultaneously Comprising Antiviral and Antibacterial Components. *Cryst. Growth Des.* **2020**, *20*, 3236−3246.
(34) Nugrahani, I.; Asyarie, S.; Soewandhi, S. N.; Ibrahim, S. The Antibiotic Potency of Amoxicillin-Clavulanate Co-Crystal. *Int. J. Pharmacol.* **2007**, *3*, 475−481.
(35) Bhatt, P. M.; Azim, Y.; Thakur, T. S.; Desiraju, G. R. Co-Crystals of the Anti-HIV Drugs Lamivudine and Zidovudine. *Cryst. Growth Des.* **2009**, *9*, 951−957.
(36) Almansa, C.; Mercè, R.; Tesson, N.; Farran, J.; Tomàs, J.; Plata-Salamán, C. R. Co-crystal of Tramadol Hydrochloride−Celecoxib (ctc): A Novel API−API Co-crystal for the Treatment of Pain. *Cryst. Growth Des.* **2017**, *17*, 1884−1892.
(37) Theuretzbacher, U. Global antibacterial resistance: The never-ending story. *J. Glob. Antimicrob. Resist.* **2013**, *1*, 63−69.
(38) Levy, S. B.; Marshall, B. Antibacterial resistance worldwide: causes, challenges and responses. *Nat. Med.* **2004**, *10*, S122−S129.
(39) Brown, E. D.; Wright, G. D. Antibacterial drug discovery in the resistance era. *Nature* **2016**, *529*, 336−343.
(40) de Kraker, M. E.; Davey, P. G.; Grundmann, H. Mortality and hospital stay associated with resistant Staphylococcus aureus and Escherichia coli bacteremia: estimating the burden of antibiotic resistance in Europe. *PLoS Med.* **2011**, *8*, e1001104.
(41) Li, X.; Bai, H.; Yang, Y.; Yoon, J.; Wang, S.; Zhang, X. Supramolecular Antibacterial Materials for Combatting Antibiotic Resistance. *Adv. Mater.* **2018**, *31*, 1805092.
(42) Payne, D. J.; Gwynn, M. N.; Holmes, D. J.; Pompliano, D. L. Drugs for bad bugs: confronting the challenges of antibacterial discovery. *Nat. Rev. Drug Discovery* **2007**, *6*, 29−40.
(43) Shemchuk, O.; Braga, D.; Grepioni, F.; Turner, R. J. Co-crystallization of antibacterials with inorganic salts: paving the way to activity enhancement. *RSC Adv.* **2020**, *10*, 2146−2149.
(44) Carpenter, M. S.; Easter, W. M. The Isopropyl Cresols. *J. Org. Chem.* **1955**, *20*, 401−411.
(45) Healy, A. M.; Worku, Z. A.; Kumar, D.; Madi, A. M. Pharmaceutical solvates, hydrates and amorphous forms: A special emphasis on cocrystals. *Adv. Drug Delivery Rev.* **2017**, *117*, 25−46.
(46) Morissette, S. L.; Almarsson, O.; Peterson, M. L.; Remenar, J. F.; Read, M. J.; Lemmo, A. V.; Ellis, S.; Cima, M. J.; Gardner, C. R. High-throughput crystallization: polymorphs, salts, co-crystals and solvates of pharmaceutical solids. *Adv. Drug Delivery Rev.* **2004**, *56*, 275−300.
(47) Grepioni, F.; Braga, D.; Chelazzi, L.; Shemchuk, O.; Maffei, P.; Sforzini, A.; Viscomi, G. C. Improving solubility and storage stability of rifaximin via solid-state solvation with Transcutol®. *CrystEngComm* **2019**, *21*, 5278−5283.
(48) Li, K. K.; Yin, S. W.; Yang, X. Q.; Tang, C. H.; Wei, Z. H. Fabrication and characterization of novel antimicrobial films derived from thymol-loaded zein-sodium caseinate (SC) nanoparticles. *J. Agric. Food Chem.* **2012**, *60*, 11592−11600.
(49) Nieto, G. Biological Activities of Three Essential Oils of the Lamiaceae Family. *Medicines (Basel)* **2017**, *4*, 63.
(50) Bassole, I. H.; Juliani, H. R. Essential oils in combination and their antimicrobial properties. *Molecules* **2012**, *17*, 3989−4006.
(51) Kim, J. M.; Marshall, M. R.; Cornell, J. A.; Preston, J. F., III; Wei, C. I. Antibacterial activity of carvacrol, citral, and geraniol against Salmonella typhimurium in culture medium and on fish cubes. *J. Food Sci.* **1995**, *60*, 1364−1368.
(52) Marchese, A.; Orhan, I. E.; Daglia, M.; Barbieri, R.; Di Lorenzo, A.; Nabavi, S. F.; Gortzi, O.; Izadi, M.; Nabavi, S. M. Antibacterial and antifungal activities of thymol: A brief review of the literature. *Food Chem.* **2016**, *210*, 402−414.
(53) Falcone, P.; Speranza, B.; Del Nobile, M. A.; Corbo, M. R.; Sinigaglia, M. A study on the antimicrobial activity of thymol intended as a natural preservative. *J. Food Prot.* **2005**, *68*, 1664−1670.
(54) Valero, D.; Valverde, J. M.; Martinez-Romero, A.; Guillen, F.; Castillo, S.; Serrano, M. The combination of modified atmosphere packaging with eugenol or thymol to maintain quality, safety and functional properties of table grapes. *Postharvest Biol. Technol.* **2006**, *41*, 317−327.
(55) Altieri, C.; Speranza, B.; Del Nobile, M. A.; Sinigaglia, M. Suitability of bifidobacteria and thymol as biopreservatives in

https://dx.doi.org/10.1021/acs.cgd.0c00900
Cryst. Growth Des. 2020, 20, 6796−6803

extending the shelf life of fresh packed plaice fillets. *J. Appl. Microbiol.* **2005**, *99*, 1294−1302.
(56) Persico, P.; Ambrogi, V.; Carfagna, C.; Cerruti, P.; Ferrocino, I.; Mauriello, G. Nanocomposite Polymer Films Containing Carvacrol for Antimicrobial Active Packaging. *Polym. Eng. Sci.* **2009**, *49*, 1447−1455.
(57) https://www.ema.europa.eu/en/human-regulatory/herbal-medicinal-products.
(58) Ash, M., *Handbook of preservatives*. ed.; Synapse Info Resources: 2004; carvacrol, p 576; thymol, p 1034.
(59) Flavor and Extract Manufacturers Association of the United States: "The safety standard applied by the FEMA Expert Panel is the same standard required by FDA, i.e. a "reasonable certainty of no harm." The FEMA Expert Panel only evaluates substances for GRAS status that are used to formulate flavors to be added to human foods. The Expert Panel does not evaluate food ingredients with functions other than flavoring nor does it evaluate flavorings for use in products other than human food." See https://www.femaflavor.org/gras.
(60) Mazzeo, P. P.; Carraro, C.; Monica, A.; Capucci, D.; Pelagatti, P.; Bianchi, F.; Agazzi, S.; Careri, M.; Raio, A.; Carta, M.; Menicucci, F.; Belli, M.; Michelozzi, M.; Bacchi, A. Designing a Palette of Cocrystals Based on Essential Oil Constituents for Agricultural Applications. *ACS Sustainable Chem. Eng.* **2019**, *7*, 17929−17940.
(61) Degen, T.; Sadki, M.; Bron, E.; Konig, U.; Nenert, G. The HighScore suite. *Powder Diffr.* **2014**, *29*, S13−S18.
(62) Altomare, A.; Cuocci, C.; Giacovazzo, C.; Moliterni, A.; Rizzi, R.; Corriero, N.; Falcicchio, A. EXPO2013: a kit of tools for phasing crystal structures from powder data. *J. Appl. Crystallogr.* **2013**, *46*, 1231−1235.
(63) Cohelo, A. *TOPAS-Academic*; Coelho Software: Brisbane, Australia, 2007.
(64) Sheldrick, G. M. SHELXT - integrated space-group and crystal-structure determination. *Acta Crystallogr., Sect. A: Found. Adv.* **2015**, *71*, 3−8.
(65) Sheldrick, G. M. Crystal structure refinement with SHELXL. *Acta Crystallogr., Sect. C: Struct. Chem.* **2015**, *71*, 3−8.
(66) Dolomanov, O. V.; Bourhis, L. J.; Gildea, R. J.; Howard, J. A. K.; Puschmann, H. OLEX2: a complete structure solution, refinement and analysis program. *J. Appl. Crystallogr.* **2009**, *42*, 339−341.
(67) Macrae, C. F.; Edgington, P. R.; McCabe, P.; Pidcock, E.; Shields, G. P.; Taylor, R.; Towler, M.; van De Streek, J. Mercury: visualization and analysis of crystal structures. *J. Appl. Crystallogr.* **2006**, *39*, 453−457.
(68) Clinical and Laboratory Standards Institute. *Performance standards for antimicrobial susceptibility testing; sixteenth informational supplement*, CLSI document M100-S16CLSI; CLSI: Wayne, PA, 2006.
(69) European Committee for Antimicrobial Susceptibility Testing (EUCAST) of the European Society of Clinical Microbiology and Infectious Diseases (ESCMID). Determination of minimum inhibitory concentrations (MICs) of antibacterial agents by broth dilution. *Clin. Microbiol. Infect.* **2003**, *9*, ix−xv.
(70) Wiegand, I.; Hilpert, K.; Hancock, R. E. Agar and broth dilution methods to determine the minimal inhibitory concentration (MIC) of antimicrobial substances. *Nat. Protoc.* **2008**, *3*, 163−175.
(71) Mazzeo, P. P.; Canossa, C.; Carraro, C.; Pelagatti, P.; Bacchi, A. Systematic coformer contribution to cocrystal stabilization: energy and packing trends. *CrystEngComm* **2020**, DOI: 10.1039/D0CE00291G.
(72) Thozet, A.; Perrin, M. Structure of 2-isopropyl-5-methylphenol (thymol). *Acta Crystallogr., Sect. B: Struct. Crystallogr. Cryst. Chem.* **1980**, *36*, 1444−1447.

https://dx.doi.org/10.1021/acs.cgd.0c00900
Cryst. Growth Des. 2020, 20, 6796−6803